ChemComm

COMMUNICATION

View Article Online
View Journal | View Issue

Cite this: *Chem. Commun.*, 2023, 59, 2461

Received 26th October 2022,
Accepted 31st January 2023

DOI: 10.1039/d2cc05800f

rsc.li/chemcomm

Converting an amorphous covalent organic polymer to a crystalline covalent organic framework mediated by a repairing agent†

Xiang-Hao Han, Rong-Ran Liang, Zhi-Bei Zhou, Qiao-Yan Qi and Xin Zhao *

We herein report a new approach to converting an amorphous covalent organic polymer to a crystalline heteropore covalent organic framework (COF), which is promoted by using an additive for structure repair. This provides a new method for the construction of COFs from cross-linked polymers.

Covalent organic frameworks (COFs) are a class of crystalline porous organic polymers typically synthesized through polycondensation of small organic molecules with matched symmetries.[1] They have been exploited in a variety of applications including gas storage,[2] separation,[3] catalysis,[4] sensing,[5] environmental remediation,[6] energy storage,[7] proton conduction,[8] and so on. Compared with amorphous porous organic materials, COFs possess pre-designed skeletons, well-defined pore structures, and accurate distribution of functional sites. These advantages are benefitted from their crystalline structures, the formation of which has been revealed through a "self-healing/error correction" process enabled by the dynamic feature of the covalent bonds (linkages) used to construct COFs,[9] typically, –B–O- and –C═N–. And it has also been established to be a general mechanism to produce crystalline COFs from initially generated amorphous networks.[10] However, despite the "self-healing/error correction" mechanism providing the basis for the formation of well-ordered frameworks, successful construction of a pre-designed COF cannot always be ensured.

On the other hand, the dynamic feature of linkages has also been exploited to improve the crystallinity of COFs. For example, conducting polycondensation reactions in the presence of monofunctional molecules was proved to be an effective approach to improving the quality of COF materials. Using monoboronic acids as modulating agents, Bein and co-workers have realized the synthesis of COFs with extremely high crystallinity and increased domain sizes.[11] In another example reported by Wang, Sun, Yaghi, and their teams, aniline was employed as a nucleation inhibitor to grow large single crystals of 3D COFs based on imine exchange.[12] Moreover, Wang *et al.* demonstrated that aniline and benzaldehyde could be used as monofunctional competitors to control the morphologies of COFs by reversibly terminating/activating the polycondensation reactions between monomers.[13] In addition, small chiral molecules as chiral inducers have been reported for the construction of chiral COFs.[14] In these examples, the monofunctional molecules are present during the polycondensations of the monomers and thus exert an influence on the reactions and structures. In this communication, we demonstrate that monofunctional molecules can also work as repairers to promote conversion from amorphous covalent organic polymers (COPs) to crystalline COFs, which can be a new method to prepare COFs from their premade polymeric precursors. In this approach, the additive small molecules play a different role from that in the previous works by working as repairing agents to repair structurally disordered cross-linked polymers into crystalline COFs.

To demonstrate this concept, an imine-based amorphous COP (named COP-DTAD) was synthesized as a precursor to explore its transformation from an amorphous network to a crystalline framework (Scheme 1). It was prepared as a yellow lumpy solid in one-pot *via* a "two-in-one" strategy,[15] based on the self-condensation of a bifunctional monomer (4,4′-((4″,5′-diamino-[1,1′:3′,1″-terphenyl]-4-yl)azanediyl)dibenzaldehyde, DTAD) which formed *via* Suzuki coupling reaction between compound **1** and compound **2** (Scheme 1A).

We selected aniline as a repairing agent to evaluate the growth of the COF (named COF-DTAD) *via* structure repairing of amorphous COP-DTAD (Scheme 1B). The COP-to-COF transformation experiment was conducted by introducing different equivalents of aniline into suspensions of COP-DTAD in *o*-dichlorobenzene/*n*-butanol/acetic acid (aq., 6 M) (5/5/1, v/v/v) in glass ampoules and then keeping the sealed ampoules at 120 °C for 72 h, which afforded repaired products as orange powders (Fig. S1, ESI†).

Key Laboratory of Synthetic and Self-Assembly Chemistry for Organic Functional Molecules, Center for Excellence in Molecular Synthesis, Shanghai Institute of Organic Chemistry, University of Chinese Academy of Sciences, Chinese Academy of Sciences, 345 Lingling Road, Shanghai 200032, China. E-mail: xzhao@sioc.ac.cn

† Electronic supplementary information (ESI) available: Materials and methods, synthesis of the COPs and the COF, and additional characterization. See DOI: https://doi.org/10.1039/d2cc05800f

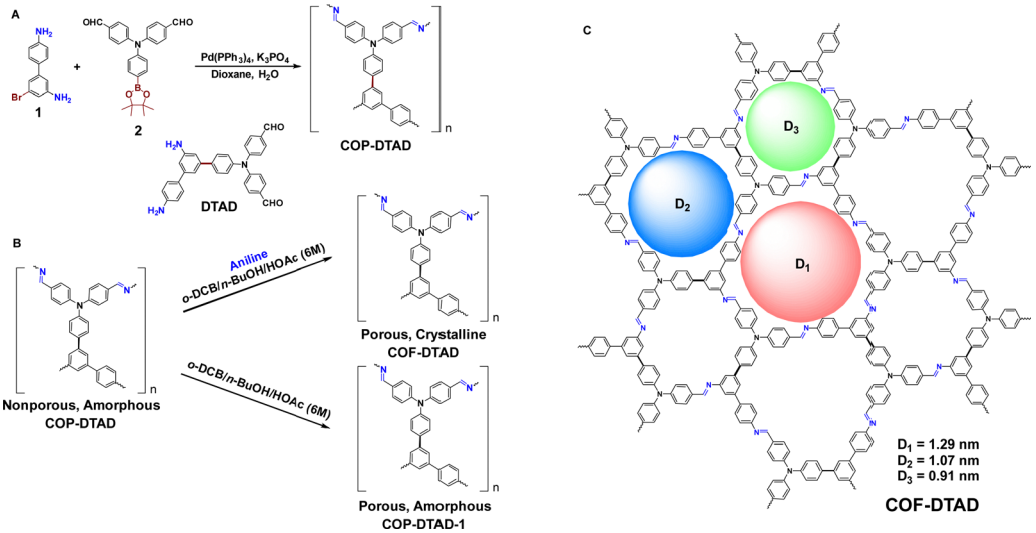

Scheme 1 Illustration of the aniline-mediated structure conversion from COP-DTAD to COF-DTAD and the preparation of COP-DTAD-1. (A) Schematic diagram of one-pot synthesis of COP-DTAD. (B) Schematic diagram of the preparation of COF-DTAD and COP-DTAD-1. (C) Illustration of the structure of COF-DTAD, which bears three different kinds of pores.

The PXRD patterns and FT-IR spectra of the polymers before and after the transformation were recorded and compared. As revealed by the PXRD results (Fig. 1a and Fig. S2 and S3, and Table S1, ESI†), for the entry without the addition of aniline, the product is still amorphous (named COP-DTAD-1). This result clearly suggests that the "self-healing/error correction" process did not come into effect under this condition. However, once aniline is introduced into the suspensions of COP-DTAD as a repairing agent, conversion of amorphous COP to crystalline COF could be achieved (Fig. 1a). Detailed study revealed that the addition of 0.5 equivalent of aniline resulted in a product with weak diffraction peaks corresponding to the (100) and (110) facets of COF-DTAD, indicating that 0.5 equivalent of aniline works as a repairer but it is not optimal for the conversion. It was further found that excessive aniline was beneficial for the formation of COF materials with high crystallinity, as revealed by the observation of the growing intensity of the PXRD peaks with increasing amounts of aniline. Moreover, the comparison of their FT-IR spectra indicates that the as-obtained polymers exhibit quite similar peaks (Fig. 1b), suggesting that they possess almost the same chemical composition. It is reasonable because they are polyimines prepared from the same monomer and the main distinction between them is different crystallinity.

To further shed light on the repair process, a time-dependent transformation experiment was carried out. Experimentally, 4 equivalents of aniline were added into suspensions of COP-DTAD in *o*-dichlorobenzene/*n*-butanol/acetic acid (aq., 6M) (5/5/1, v/v/v) and the mixtures were heated at 120 °C for 2, 4, 8, 12, and 24 hours, respectively. As shown in Fig. 2a, the PXRD analysis reveals that the characteristic peaks (2θ = 3.38° and 5.87°) of COF-DTAD become visible at 4 h and their intensities increase with the elongation of the reaction time. After 12 h, a crystalline COF material is produced. Extending the reaction time to 24 h leads to higher intensity of the main diffraction peak, and the intensity of the diffraction peaks does not exhibit further enhancement after 48 h (Fig. S4, ESI†). Similar to the above results observed for the addition of different equivalents of aniline, the FT-IR spectra of the products of different conversion time just show slight changes (Fig. 2b),

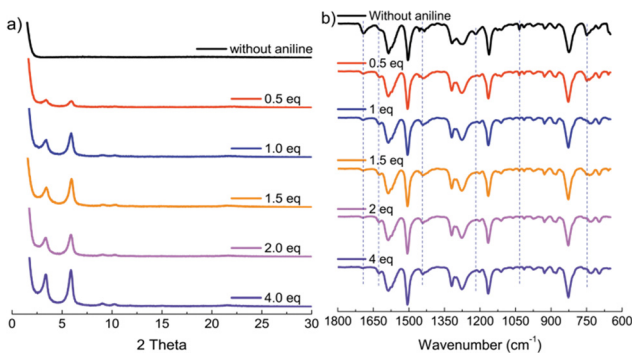

Fig. 1 (a) PXRD patterns and (b) FT-IR spectra of COF-DTAD prepared by heating mixtures of COP-DTAD with different equivalents of aniline for 72 h at 120 °C.

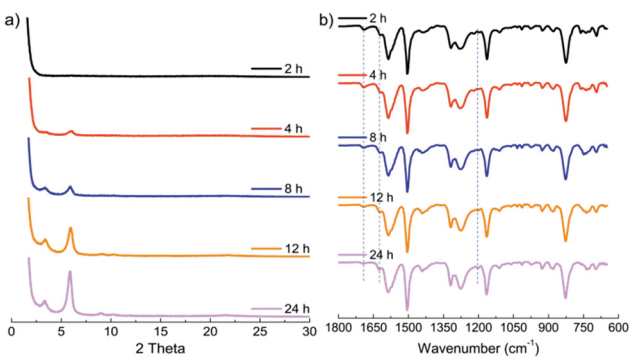

Fig. 2 (a) PXRD patterns and (b) FT-IR spectra of COF-DTAD converted from COP-DTAD at different time intervals.

again indicating their same chemical composition. These results further indicate that aniline can effectively promote the COP-to-COF transformation. The mechanism is proposed to be a result of imine exchange: aniline breaks some of the imine bonds in the premade COP by forming new imine bonds between it and the DTAD unit. As a result, free amino groups of DTAD are released from the amorphous COP, which sequentially initiates structure reconstruction of the COP by reconnecting the monomer unit *via* re-formation of imine bonds between them and releasing aniline again. In such a way, the undesired connections which result in the amorphous network of COP-DTAD are corrected to produce the crystalline COF during the imine exchange process (Scheme S1, ESI†).

The comparison of the porosity and surface area before and after the conversion also supports the key role of aniline in the repair process. The permanent porosity and surface areas of COP-DTAD and COF-DTAD were assessed by nitrogen adsorption analysis at 77 K (Fig. 3a and Fig. S5a, ESI†). For COP-DTAD, a very low N_2 uptake and a negligible Brunauer–Emmett–Teller (BET) surface area ($\sim$1 $m^2\ g^{-1}$) were obtained (Fig. S5b, ESI†), indicating a nonporous characteristic. In sharp contrast, COF-DTAD shows a high N_2 uptake and its adsorption–desorption isotherm fits the type I sorption model with a rapid N_2 uptake at the low relative pressure range ($P/P_0 < 0.05$), indicating the permanent microporous feature of the COF.[16] Its BET surface area was calculated to be 1120 $m^2\ g^{-1}$ and the total pore volume (at P/P_0 = 0.99) was 0.58 $cm^3\ g^{-1}$ (Fig. S5c, ESI†). Pore size distribution (PSD) analysis reveals that COF-DTAD displays three distribution peaks around 8.0, 10.0, and 11.8 Å, respectively (Fig. 3b). These values are consistent with the theoretical pore sizes of the three different kinds of pores in the proposed triple-pore COF (9.1, 10.7, and 12.9 Å, Scheme 1C), as estimated by Zeo++calculations (Fig. S6, ESI†),[17] corroborating again that the irregular structure of the amorphous COP was repaired to give rise to the crystalline COF with well-ordered internal microstructure. On the other hand, COF-DTAD-1, which was prepared by heating a suspension of COP-DTAD under the same solvent conditions but without aniline, exhibits a BET surface area of 860 $m^2\ g^{-1}$, much higher than that of COP-DTAD (Fig. S7, ESI†), albeit it is still amorphous. This result suggests that this solvothermal treatment of nonporous COP-DTAD results in partial "self-healing/error correction", but cannot completely repair the amorphous COP structure into a crystalline framework without the assistance of the repairing agent aniline.

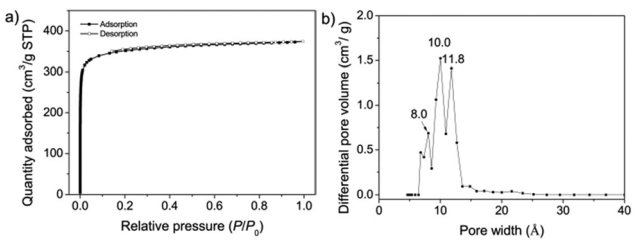

Fig. 3 (a) N_2 adsorption–desorption isotherm (77 K) and (b) PSD profile of COF-DTAD.

The as-prepared polyimines, including both the amorphous COPs and the crystalline COF were characterized by a variety of methods. Firstly, the comparison of the FT-IR spectra between them and the starting materials confirms the composition of the polymers. The isolated polymers show significant loss of the peaks corresponding to –C(O)–H (2827 cm^{-1} and 2737 cm^{-1} of compound **2**), –C═O (1686 cm^{-1} of compound **2**), and –NH_2 (3437–3205 cm^{-1} of compound **1**) (Fig. S8, ESI†), indicating high completion degrees of the condensation reactions. Moreover, the appearance of the peaks corresponding to –C═N– vibration bands could be identified at 1625 cm^{-1} in the polymers, further confirming the formation of polyimines. It should be noted that the peaks corresponding to the –C═O vibration could still be observed in the IR spectra of the polyimines, which could be attributed to the terminal aldehyde group at their edges. The formation of the polyimine structure was also indicated by solid-state cross-polarization with magic angle spinning (CP/MAS) ^{13}C NMR spectroscopy, which exhibits a resonance signal at 155 ppm for COF-DTAD, corresponding to the chemical shift of the newly formed –C═N– bond (Fig. S9, ESI†). Elemental analysis indicates that the contents of C, H, and N of COF-DTAD are closer to the corresponding theoretical values than those of the COPs (see Supporting Information for details). This might be due to fewer defects in the crystalline COF in comparison with the amorphous COPs. Thermogravimetric analysis (TGA) reveals that all three polyimines exhibit good thermal stability and COF-DTAD was the best one (Fig. S10, ESI†). The chemical stability of COF-DTAD was examined, which showed its good resistance to acid (Fig. S11, ESI†). Scanning electron microscopy (SEM) reveals that the amorphous and crystalline polyimines display different morphologies, with COF-DTAD consisting of aggregation of relatively regular microspheres, while COP-DTAD exhibits a lumpy structure with a rough surface (Fig. S12 and S13, ESI†). Interestingly, COP-DTAD-1 displays a morphology of random distribution of microspheres on a lumpy structure, like a hybrid structure of COF-DTAD and COP-DTAD (Fig. S14, ESI†).

In order to determine the crystal structure of COF-DTAD, its powder X-ray diffraction (PXRD) pattern was further analyzed by comparison with the simulated PXRD patterns of the theoretically predicted structures for 2D COFs with three different kinds of pores (Fig. 4c and e).[18] As shown in Fig. 4a, the experimental PXRD pattern of COF-DTAD displays two strong peaks at 3.38° and 5.87°, along with weak peaks at 8.98° and 10.19°, which are assigned to the (100), (110), (210), and (300) facets, respectively. Another four peaks with quite low intensities could also be observed under amplification, which appear at 11.77°, 13.61°, 19.71°, and 21.48°, assignable to (220), (400), (320), and (001) facets, respectively. Pawley refinement was conducted to output the optimized unit-cell parameters of COF-DTAD, which are $a = b$ = 29.98 Å, c = 4.13 Å, $\alpha = \beta = 90°$, $\gamma = 120°$, with R_{wp} = 5.52% and R_p = 3.81% (Tables S2 and S3, ESI†). The difference plot between the experimental and refined diffraction patterns indicates a high consistency between them (Fig. 4b). In addition, a structure with a staggered stacking model was also simulated (Fig. 4f). However, it was ruled out to

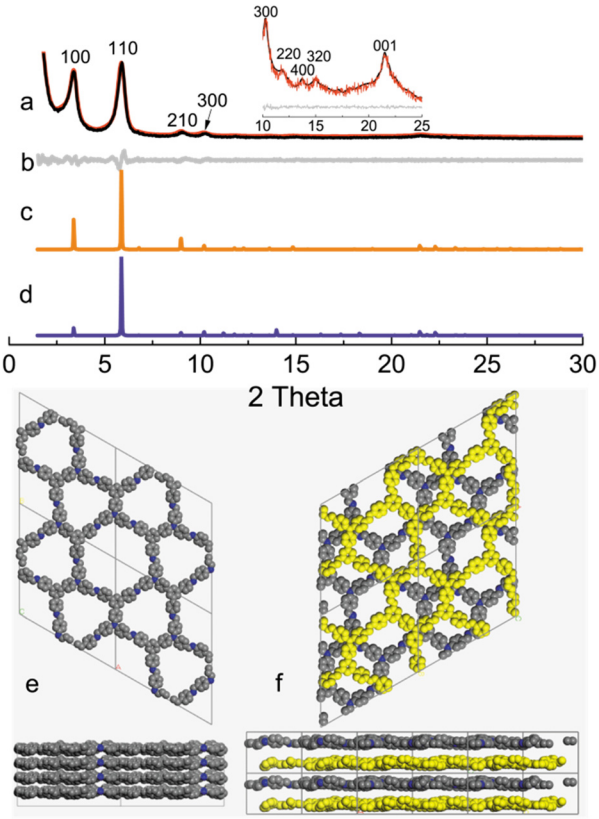

Fig. 4 TOP: (a) Experimental (black) and refined (red) PXRD patterns of COF-DTAD. (b) Difference plot (grey) between the experimental and refined PXRD patterns. Simulated PXRD patterns for (c) eclipsed (orange) and (d) staggered (violet) structures. Bottom: Perspective and top views of structural representation of COF-DTAD in (e) eclipsed and (f) staggered stacking.

be the product of the COP-to-COF transformation because of the significant deviation in relative intensity between the experimental and simulated PXRD peaks (Fig. 4d).

In summary, we have shown a novel structure repairing phenomenon in the transformation of an amorphous nonporous COP to a crystalline COF, which is mediated by introducing a monofunctional molecule as a repairing agent. Promoted by the repairing agent (aniline in this work), the amorphous COP is successfully converted into a heteropore COF with three-level hierarchical porosity. This work offers a new method to synthesize COFs or improve their crystallinity, which could be applicable to the COFs hard to construct *via* a self-healing process.

We thank the National Natural Science Foundation of China (21725404) and the Science and Technology Commission of Shanghai Municipality (20JC1415400) for financial support.

Conflicts of interest

There are no conflicts of interest to declare.

Notes and references

1 (*a*) K. Geng, T. He, R. Liu, S. Dalapati, K. T. Tan, Z. Li, Y. Gong, Q. Jiang and D. Jiang, *Chem. Rev.*, 2020, **120**, 8814–8933; (*b*) R.-R. Liang, S.-Y. Jiang, A. Ru-Han and X. Zhao, *Chem. Soc. Rev.*, 2020, **49**, 3920–3951; (*c*) X. Guan, F. Chen, Q. Fang and S. Qiu, *Chem. Soc. Rev.*, 2020, **49**, 1357–1384.

2 (*a*) S. S. Han, H. Furukawa, O. M. Yaghi and W. A. Goddard, *J. Am. Chem. Soc.*, 2008, **130**, 11580–11581; (*b*) Z. Li, X. Feng, Y. Zou, Y. Zhang, H. Xia, X. Liu and Y. Mu, *Chem. Commun.*, 2014, **50**, 13825–13828; (*c*) Q. Gao, X. Li, G.-H. Ning, H.-S. Xu, C. Liu, B. Tian, W. Tang and K. P. Loh, *Chem. Mater.*, 2018, **30**, 1762–1768; (*d*) Y. Zeng, R. Zou and Y. Zhao, *Adv. Mater.*, 2016, **28**, 2855–2873.

3 (*a*) K. Dey, M. Pal, K. C. Rout, S. Kunjattu H, A. Das, R. Mukherjee, U. K. Kharul and R. Banerjee, *J. Am. Chem. Soc.*, 2017, **139**, 13083–13091; (*b*) B. Tang, W. Wang, H. Hou, Y. Liu, Z. Liu, L. Geng, L. Sun and A. Luo, *Chin. Chem. Lett.*, 2022, **33**, 898–920; (*c*) Z. Wang, S. Zhang, Y. Chen, Z. Zhang and S. Ma, *Chem. Soc. Rev.*, 2020, **49**, 708–735.

4 (*a*) S.-Y. Ding, J. Gao, Q. Wang, Y. Zhang, W.-G. Song, C.-Y. Su and W. Wang, *J. Am. Chem. Soc.*, 2011, **133**, 19816–19822; (*b*) X. Wang, X. Han, J. Zhang, X. Wu, Y. Liu and Y. Cui, *J. Am. Chem. Soc.*, 2016, **138**, 12332–12335; (*c*) A. Jati, K. Dey, M. Nurhuda, M. A. Addicoat, R. Banerjee and B. Maji, *J. Am. Chem. Soc.*, 2022, **144**, 7822–7833; (*d*) X.-T. Li, J. Zou, Q. Yu, Y. Liu, J.-R. Li, M.-J. Li, H.-C. Ma, G.-J. Chen and Y.-B. Dong, *Chem. Commun.*, 2022, **58**, 2508–2511.

5 (*a*) Z. Li, Y. Zhang, H. Xia, Y. Mu and X. Liu, *Chem. Commun.*, 2016, **52**, 6613–6616; (*b*) F.-Z. Cui, J.-J. Xie, S.-Y. Jiang, S.-X. Gan, D.-L. Ma, R.-R. Liang, G.-F. Jiang and X. Zhao, *Chem. Commun.*, 2019, **55**, 4550–4553; (*c*) G. Lin, H. Ding, D. Yuan, B. Wang and C. Wang, *J. Am. Chem. Soc.*, 2016, **138**, 3302–3305.

6 (*a*) Q. Sun, B. Aguila, J. Perman, L. D. Earl, C. W. Abney, Y. Cheng, H. Wei, N. Nguyen, L. Wojtas and S. Ma, *J. Am. Chem. Soc.*, 2017, **139**, 2786–2793; (*b*) N. Liu, L. Shi, X. Han, Q.-Y. Qi, Z.-Q. Wu and X. Zhao, *Chin. Chem. Lett.*, 2020, **31**, 386–390; (*c*) S. Zhuang, Y. Liu and J. Wang, *J. Hazard. Mater.*, 2020, **383**, 121126.

7 (*a*) C. R. DeBlase, K. E. Silberstein, T. Thanh-Tam, H. D. Abruna and W. R. Dichtel, *J. Am. Chem. Soc.*, 2013, **135**, 16821–16824; (*b*) Y. Hu, L. J. Wayment, C. Haslam, X. Yang, S.-h Lee, Y. Jin and W. Zhang, *EnergyChem*, 2021, **3**, 100048; (*c*) J. Li, X. Jing, Q. Li, S. Li, X. Gao, X. Feng and B. Wang, *Chem. Soc. Rev.*, 2020, **49**, 3565–3604.

8 (*a*) S. Chandra, T. Kundu, S. Kandambeth, R. BabaRao, Y. Marathe, S. M. Kunjir and R. Banerjee, *J. Am. Chem. Soc.*, 2014, **136**, 6570–6573; (*b*) H. Xu, S. Tao and D. Jiang, *Nat. Mater.*, 2016, **15**, 722–726; (*c*) X.-F. Liu, S.-Z. Huang, Y.-X. Lian, X.-Y. Dong and S.-Q. Zang, *Chem. Commun.*, 2022, **58**, 6084–6087.

9 S. Kandambeth, K. Dey and R. Banerjee, *J. Am. Chem. Soc.*, 2019, **141**, 1807–1822.

10 (*a*) B. J. Smith, A. C. Overholts, N. Hwang and W. R. Dichtel, *Chem. Commun.*, 2016, **52**, 3690–3693; (*b*) W. Kong, W. Jia, R. Wang, Y. Gong, C. Wang, P. Wu and J. Guo, *Chem. Commun.*, 2019, **55**, 75–78; (*c*) X.-H. Han, J.-Q. Chu, W.-Z. Wang, Q.-Y. Qi and X. Zhao, *Chin. Chem. Lett.*, 2022, **33**, 2464–2468; (*d*) Y. Lv, Y. Li, G. Zhang, Z. Peng, L. Ye, Y. Chen, T. Zhang, G. Xing and L. Chen, *CCS Chem.*, 2022, **4**, 1519–1525; (*e*) J. Tan, S. Namuangruk, W. Kong, N. Kungwan, J. Guo and C. Wang, *Angew. Chem., Int. Ed.*, 2016, **55**, 13979–13984.

11 M. Calik, T. Sick, M. Dogru, M. Döblinger, S. Datz, H. Budde, A. Hartschuh, F. Auras and T. Bein, *J. Am. Chem. Soc.*, 2016, **138**, 1234–1239.

12 T. Ma, E. A. Kapustin, S. X. Yin, L. Liang, Z. Zhou, J. Niu, L. H. Li, Y. Wang, J. Su, J. Li, X. Wang, W. D. Wang, W. Wang, J. Sun and O. M. Yaghi, *Science*, 2018, **361**, 48–52.

13 S. Wang, Z. Zhang, H. Zhang, A. G. Rajan, N. Xu, Y. Yang, Y. Zeng, P. Liu, X. Zhang, Q. Mao, Y. He, J. Zhao, B.-G. Li, M. S. Strano and W.-J. Wang, *Matter*, 2019, **1**, 1592–1605.

14 (*a*) X. Han, J. Zhang, J. Huang, X. Wu, D. Yuan, Y. Liu and Y. Cui, *Nat. Commun.*, 2018, **9**, 1294; (*b*) F. Li, J.-L. Kan, B.-J. Yao and Y.-B. Dong, *Angew. Chem., Int. Ed.*, 2022, **61**, e202115044; (*c*) H. Chen, Z.-G. Gu and J. Zhang, *J. Am. Chem. Soc.*, 2022, **144**, 7245–7252.

15 Y. Li, Q. Chen, T. Xu, Z. Xie, J. Liu, X. Yu, S. Ma, T. Qin and L. Chen, *J. Am. Chem. Soc.*, 2019, **141**, 13822–13828.

16 M. Thommes, K. Kaneko, A. V. Neimark, J. P. Olivier, F. Rodriguez-Reinoso, J. Rouquerol and K. S. W. Sing, *Pure Appl. Chem.*, 2015, **87**, 1051–1069.

17 R. L. Martin, B. Smit and M. Haranczyk, *J. Chem. Inf. Model.*, 2012, **52**, 308–318.

18 X.-H. Han, Q.-Y. Qi, Z.-B. Zhou and X. Zhao, *Chin. J. Chem.*, 2020, **38**, 1676–1680.

